Tailored reduced kinetic mechanisms for atmospheric chemistry modeling

L. M. T. Joelsson*, C. Pichler, E. J. K. Nilsson

Department of Physics, Combustion Physics, Lund University, Box 118, SE-221 00 Lund, Sweden

Abstract

Reduced chemical kinetic mechanisms are essential for atmospheric chemistry modeling where use of explicit kinetic schemes are too computationally demanding. By tailoring of mechanisms to specific cases, mechanism size can be kept small, without significant loss of accuracy in predictions of selected species' concentrations. In the present work we present small kinetic mechanisms tailored using a novel method.

The reduced mechanisms are generated by applying the method to several cases previously described in the literature and their performance in box model simulations are evaluated. The characteristics of the reduced mechanisms are examined. In addition, the method's sensitivity towards time scales, choice of trace gas species of interest; and NO_x regime are investigated.

The reduced mechanisms include 10 %–30 % of all the reactions in the relevant subset of the detailed chemical mechanism. Simulations with the reduced mechanisms typically yield no loss in accuracy of ozone concentration predictions and less than a 10 % accuracy loss for the concentration predictions of nitrogen oxides for the cases over as long as five simulated days.

Mechanisms generated to predict the concentrations of few species, over short time scales, high NO_x conditions with no isoprene generally include fewer reactions than mechanisms generated to predict the concentrations of several

---
*Corresponding author
Email address: magnus.joelsson@forbrf.lth.se (E. J. K. Nilsson)

species, over long time scales, in isoprene rich, low NO_x conditions.

1. Introduction

Growing concern for emissions of air pollutants deteriorating local and regional air quality as well as greenhouse gases altering the Earth's radiation budget, has spurred development of computational modeling of the atmosphere (e.g. Ginnebaugh et al., 2010; Naik et al., 2013). Modeling is a tool to understand atmospheric processes and a means of predicting trends in climate and air quality by extrapolation into the future. Accurate predictions of concentrations of various trace gases are important in order to provide proper decisions basis for policy-makers, both on local and regional air quality and on global climate issues (IPCC, 2013).

Coupled atmospheric chemistry-transport modeling is conducted at a wide range of spatial scales, from global (e.g. Emmons et al., 2010) and regional scales (Monks et al., 2009) to the street scale (Zhong et al., 2016a). The scale of the model domain put requirements on the chemical kinetic mechanism, since the (advection) time scale and spatial scale of a chemistry-transport system are coupled. In the present study, time scales of up to five days are considered and extra attention is paid to the urban local scale (i.e. street canyon) application, since the coupled chemistry-transport modeling in this setting is a rather new research topic with high demands on the chemical mechanisms. Also, local systems under short periods of time will experience a narrower span of conditions than a global system under long periods of time. A local scale model will therefore be especially suitable for a tailored reduction of its chemical description.

Reduction of kinetic mechanisms is commonly achieved via structural lumping (Gery et al., 1989), intermediate species lumping (Jenkin et al., 2008), emission lumping (Stockwell et al., 1997; Watson et al., 2008; Bright et al., 2013) or sensitivity analysis (present study). Several reduced chemical mechanisms have

been presented in the literature, some described in a review of coupled street canyon modeling (Zhong et al., 2016a), some described in a comparison study of chemical mechanisms used in global models (Emmerson and Evans, 2009). The level of detail on the mechanisms vary from simple O_3–NO_x chemistry (nitrogen oxides: $[NO_x] = [NO] + [NO_2]$) to inclusion of a range of hydrocarbons.

Some street canyon air quality studies develop or use reduced mechanisms based on the Master Chemical Mechanism (MCM) family of mechanisms (Bright et al., 2013; Zhong et al., 2016b). MCM is an attempt to describe tropospheric chemistry explicitly (Saunders et al., 2003; Jenkin et al., 2003; MCM, 2018). The latest MCM version 3.3.1 (Jenkin et al., 2015) follow the photooxidation path of methane and 142 additional VOCs adding up to 16 701 reactions and 5 832 species. Other extensive mechanisms are the National Center for Atmospheric Research Master Mechanism (NCAR-MM) (Madronich and Calvert, 1989; NCAR, 2018) and the Statewide Air Pollution Research Center Atmospheric Chemical Mechanisms (SAPRC) (Carter, 2010; Carter and Heo, 2013; SAPRC, 2013). These mechanisms and more are briefly reviewed in Zhong et al. (2016a) and compared in Chen et al. (2010). The results of Chen et al. (2010) as well as of other studies (e.g. Emmerson and Carslaw, 2009; Whalley et al., 2011) indicate that no mechanism thus far is able to perfectly replicate field measurement data in any given settings nor is there necessarily always a negative correlation between deviation from measurement and mechanism size. For example, hydrogen radical concentrations in low NO_x environments have proved elusive. The limitation of the parent mechanism will presumably be inherited in any reduced mechanism. Most of the street-scale simulations use mechanisms either originally developed for regional or global applications, such as the GEOS-Chem mechanism (Kim et al., 2012), or derived from such mechanisms, e.g. Reduced Chemistry Scheme (RCS) (Bright et al., 2013; Zhong et al., 2016b) and Complex Chemical Mechanism (CCMCFD) (Sanchez et al., 2016) which are derived from the Common Representative Intermediate (CRI) (Jenkin et al., 2008) and Regional Atmospheric Chemistry Mechanism (RACM) (Stockwell et al., 1997), respectively.

When reducing mechanisms, there will always be a trade-off between accuracy and computational speed (which depend on the number of reactions and species included). A way to solve the need for accuracy but still keep the number of reactions and species low is to tailor mechanisms for a limited set of conditions with respect to emissions, concentrations, etc. Other important aspects of the tailoring procedure are the time scales for which the reduced mechanism is to be used and the compounds for which the concentrations are considered important to predict (target compounds). To our knowledge, the first automatically tailored mechanism to be used in a street canyon simulation, was CCMCFD, developed in by Sanchez et al. (2016) with the software CHEMATA (CHEmical Mechanism Adaptation to Tropospheric Applications) (Kirchner, 2005; Junier et al., 2005). CHEMATA takes species, their source strength, and kinetic data as input to generate an explicit or lumped reduced mechanism. CHEMATA does not, however, consider other conditions such as time frames, solar radiation, and temperature (solar radiation and temperature is implicitly included in the kinetic data input, but does not, to our understanding, influence the selection of reactions or species) nor does it consider the interest of the user in terms of predictions of certain compounds. These conditions constrain the degree to which a mechanism can be reduced with utility as will be shown below. Moreover, advances in kinetic research (e.g. Yarwood et al., 2010; Carter and Heo, 2013; Jenkin et al., 2015) calls for continuous updating of the detailed mechanisms, eventually making the older versions and thus their reduced offspring outdated. The tailored approach will enable the reduced mechanisms to be in pace with the most recent detailed version of its parent mechanism franchise.

The aim of the present work is to evaluate the performance and describe the characteristics of tailored kinetic mechanisms for modeling of atmospheric chemistry. Reduced mechanisms generated for cases with different compositions of trace gases, values of temperature, relative humidity, and solar radiation influx, along with various time scales and sets of target compounds are evaluated and characterized. Differences among the reduced mechanisms, which presumably reflect their cases' NO_x regime, are given special attention. From evaluation

of the mechanisms performance and characteristics, conclusions can be made
on the need for chemical detail in modeling of atmospheric chemistry. In the
current study, chemical kinetics mechanisms are tailored for six cases originally
presented by Emmerson and Evans (2009) plus one high NO_x case (see Section
2.2) along with a mechanism tailored for all six cases combined. Mechanisms are
also tailored for three time scales (see Section 2.3) and two target compound
sets (see Section 2.4). Their performance (ability to accurately predict tar-
get compound concentrations), sizes (number of reactions), and characteristics
(composition of reactions) are discussed (see Section 3).

2. Methodology

2.1. Mechanism reduction and box modeling

The kinetic mechanisms employed in the current study, are generated by
reducing a detailed mechanism (henceforth called base mechanism) while lim-
iting the consequential loss of precision of relevant predictions. Here, the base
mechanism is MCM v3.3.1. The reduction method, denoted Ant Colony Re-
duction (ACR), is a semi-stochastic, statistical method based on the heuristic
Ant Colony Optimization (ACO) concept (Dorigo et al., 1996; Dorigo and Bi-
rattari, 2011) and was recently developed for combustion physics applications
(Pichler and Nilsson, 2018). The main idea behind the ACO algorithms is to
mimic biological ant colonies' ability to find optimal trails between their anthill
and some food resource by communications via the distribution of pheromones.
Similarly, within ACR, simulated ants are set out to find optimal oxidation
paths in a kinetic mechanism from an emitted compound (e.g. VOC or NO_x) to
an oxidation end product (e.g. water vapor, carbon dioxide, or aqueous phase
nitric acid). A large number of functional reduced mechanisms are generated for
each application of the method which partly allows the users to select the most
suitable mechanism for their demands, partly allows the method to be improved
recursively. The reduced mechanisms are evaluated via box model simulations.

6

The reduction process is designed as such: All reactions in the base mechanism with one particular species (initially, this can be an emitted hydrocarbon) as reactant are listed. The reactions are ascribed weights calculated from a combination of static rate of production values and non-static "pheromone"-values. The pheromone-value mimic the ant's pheromone trails, which intensities are used to communicate the utility of a certain path from the anthill to a food resource between individual ants and the ant colony. Thus, the artificial pheromone-value in the method is continuously re-calculated based on feedback data from the method itself (e.g. reduced mechanism performance and size).

Reactions important for an accurate description on the chemical system will hence gain more weight through the reduction process compared to less important reactions. A reaction is semi-stochastically selected according to their weight; this way an entire oxidation path is built up. The set of reactions collected through the process makes up the reduced mechanism. The reduced mechanism is evaluated by a box model simulation and is given an (average) root-mean-square score, see Eq. (1).

The accuracy (or score) of the mechanisms is defined as:

$$\text{score} \equiv \frac{1}{n} \sum_{A=X_1, X_2, \ldots, X_n} 1 - \sqrt{\left(\frac{[A]_{\text{reduced}}}{[A]_{\text{base}}} - 1 \right)^2} \tag{1}$$

where [A] is the concentration of target compound A. The subscript *reduced* refers to predictions obtained with a simulation using the reduced mechanism, in this case the subscript *base* refers to predictions (base predictions) obtained with a simulation using the base mechanism, but can also be concentrations obtained with measurements.

The box model used in the current study is a version of the chemical module of the Aerosol Dynamics, gas- and particle-phase chemistry model for laboratory CHAMber studies (ADCHAM) model (Roldin et al., 2014), where the aerosol sub-module is omitted. The model uses the Kinetic Pre-Processor (KPP) software (Damian et al., 2002). The photolysis constants are calculated with the Tropospheric Ultraviolet and Visible (TUV) Radiation Model (NCAR, 2018).

In the process, a large number of reduced mechanisms (here, 6 000) are con-

structed and evaluated before one final reduced mechanisms is selected. Note

that all the constructed reduced mechanisms are functional kinetic mechanisms

even though the primary role of this abundancy in mechanism generation and

scoring is to refine the overall reduction process. The reduced mechanisms span

a range of sizes and corresponding accuracy, such that either a sufficiently small

(inexpensive) or sufficiently accurate mechanism for the demand of the appli-

cation in question can be chosen. In the current study, the smallest (including

fewest reactions) reduced mechanism scoring higher than 0.9 (0.7 for the *biogenic*

case, see below) is selected. This reduced mechanism is called A0.90 (A0.70).

The entire process takes a few hours on the working desk-top machine used in

the present work (15.7 GB memory, eight-core processor $\times 16$), depending on

the complexity of the case.

Example of full selections of accepted reduced mechanisms generated by

entire reduction processes and the selected reduced mechanisms are depicted in

Fig. 1.

2.2. Cases: Different pollution scenarios

Mechanisms are generated for the prediction of the target compound sets

described below (see Section 2.4) in six cases, previously described by Emmerson

and Evans (2009).

The initial conditions for the six cases are derived from an annual simula-

tion of the GEOS-CHEM composition transport model (Bey et al., 2001). The

six cases take on values from grid boxes which reach extremes in typical tracer

concentration patterns representing six types of environments: *Industrial, clean,*

cold & dry, hot & wet, biogenic, and *non-biogenic*. The initial values of the six

cases are tabulated in Table 1. The cases were used to study the six chemistry

mechanisms' ability to predict the concentrations of ozone, NO_x, nitrate, hy-

droxyl radical, and PAN for five simulated days (120 hour), starting at midnight

local time, in a box model setting. Emmerson and Evans' idea is to test the

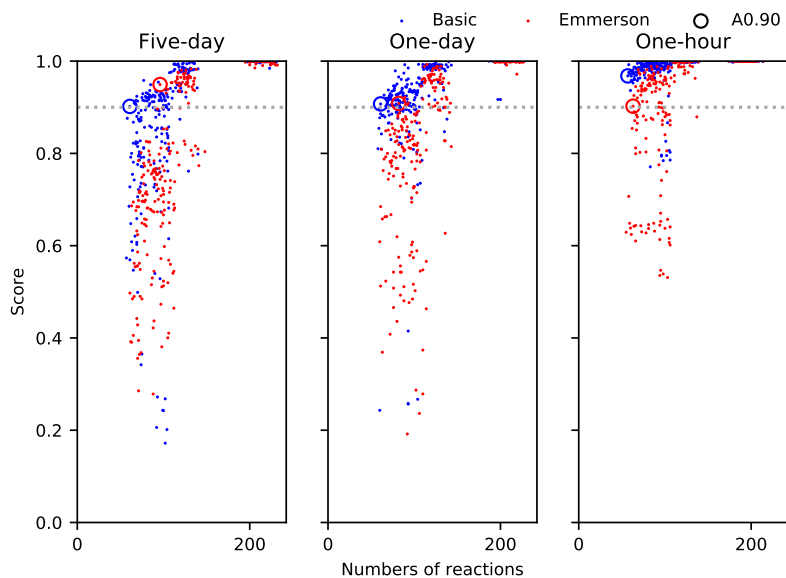mechanisms in the wide range of condition which are likely to occur in a global

Figure 1: The full selection of accepted mechanisms generated by six entire reduction processes of the *hot & wet* case, see Table 1. Mechanisms tuned to the three different time scale are depicted in the three panels (from left to right): Five-day, one-day, and one-hour. Mechanisms tuned to the two target compound sets are depicted with colored dots: *Basic* (blue) and *Emmerson* (red). The A0.90 mechanisms are encircled, the grey dotted lines correspond to the cut-off for the score (0.90).

model. In the current study, the idea is to test the method's ability to tailor
175   mechanisms for this wide range of realistic (but simplified) conditions, and to
evaluate the inter-variability of the produced mechanisms for the six cases. The
five-day time scale and the target compounds are retained in the current study.
Emmerson and Evans (2009) use MCM v3.1 as the benchmark. The mean devi-
ation of the target compounds between MCM v3.1 and MCM v3.3.1 formulated
180   as a score with the MCM v3.3.1 used as the base mechanism for all the cases
lie between 0.44 and 0.89, reflecting the development of the MCM mechanism.
Direct comparisons between the current simulation results and the benchmark
simulation of Emmerson and Evans (2009) are thus not relevant. The mean
deviation of the target compounds between MCM v3.1 and MCM v3.3.1 formu-

lated as a score with the MCM v3.3.1 used as the base mechanism for all the cases are presented in Section S.1 and the time resolved predictions are plotted in Figs. S.1–S.6 in the Supplementary Material.

Two cases include isoprene (C_5H_8, *industrial* and *biogenic*) and four do not. The four non-isoprene cases all share the same initial compound setup, only the initial concentrations of the different compounds are varied. Similarly, the two isoprene cases share the same initial compound setup. The four non-isoprene cases will thus be reduced from (and tested against) one particular subset of the full MCM mechanism (296 reactions, 99 species), and the two isoprene cases will be reduced from another particular subset (2016 reactions, 638 species). The non-isoprene base mechanism corresponds to a MCM subset with methane, ethane, propane, formaldehyde, acetaldehyde, and acetone as parent compounds including inorganic species as can be downloaded from the MCM website (MCM, 2018). All reaction including sulphur are removed. The isoprene base mechanism corresponds to a MCM subset which includes isoprene as well as all the other parent compounds listed above. There is a substantial complexity of the isoprene chemistry (Jenkin et al., 2015; Wennberg et al., 2018); the isoprene chemistry subset covers 1 900 reactions, which is about 10 % of the size of the full MCM mechanism. Furthermore, isoprene's two olefinic bonds warrant high reactivity and thus a significant role in ozone chemistry.

The NO_x regime of a system can be indicated by whether the dominant sink of radicals (hydroxyl-, hydroperoxyl-, and organic peroxy radicals) is reactions with NO_x or not (Jacob, 1999). Kleinman et al. (1997) introduces the measure L_N/Q as an indicator for the NO_x regime of a system, where L_N represents the total rate of all reactions where a radical reacts with either nitric oxide or nitrogen dioxide and Q the total rate of all radical loss reactions. A high NO_x system is defined as a system where $L_N/Q > 0.5$, a system with $L_N/Q < 0.5$ is defined as a low NO_x system. Consequently, a system commonly shifts from one regime to another under the course of a day. The average ratios, $\mu(L_N/Q)$, for the cases are tabulated in Table 1. It can be noted that three cases are (on average) in the high NO_x regime: *Industrial*, *cold & dry*, and *non-biogenic* and

three cases are in the low NO_x regime: *Clean*, *hot & wet*, and *biogenic*. The time resolved L_N/Q ratios for the cases are plotted in Figs. S.7–S.13 in the Supplementary Material.

In order to isolate the chemistry's sensitivity of L_N/Q, mechanisms are re-

₂₂₀ duced for the *hot & wet* case with increased levels of nitrogen dioxide, in addition to the cases represented in (Emmerson and Evans, 2009), see the high NO_x rows in Table 1. The initial concentration of 80 ppb nitrogen dioxide is chosen to be comparably high, but not unrealistic. The value is below the official 1-hour health thresholds for nitrogen dioxide, but slightly above the an-

₂₂₅ nual mean threshold: The WHO 1-hour average nitrogen dioxide standard is set to $200 \mu gm^{-3} \approx 100ppb$ and the annual nitrogen dioxide standard is set to $40 \mu gm^{-3} \approx 20ppb$ (WHO, 2006), the EPA 1-hour average nitrogen dioxide standard is set to 100 ppb and the annual average nitrogen dioxide standard is set to 53 ppb (EPA, 2011).

₂₃₀ Finally, one mechanism is generated for the purpose of predicting the target compound concentrations with (on average) high accuracy for all Emmerson and Evans' six original cases. This mechanism is named the *all-round* mechanism.

2.3. Time scales

To investigate the methods sensitivity to time scales, mechanisms are tailored

₂₃₅ to the cases described in Section 2.2 over shorter time scales. The underlying assumption is that shorter time scales offer less time for the chemistry to evolve and therefore the selection of chemical reactions may differ. Furthermore, the exclusion of a period without photolysis (night) is expected to influence the size and characteristics of a reduced mechanism.

₂₄₀ Mechanisms are generated for time scales of one day (24 hours) and one hour in addition to the default time scale of five days. One hour corresponds to the time scales of residence time in a confined urban environment that is not efficiently ventilated to the free boundary layer. An hour in the middle of the day is selected. The day time simulations are initialized at 11:30 local time such

₂₄₅ that solar zenith of the simulations will occur at the midpoint of the simulation

time, as for the simulations with longer time scales. The one-day and five-day simulations will be initialized at midnight.

When considering time scales, also the spin-up time of the model should be taken into account. The spin up allows the concentrations of all uninitialized compounds to build up to realistic levels. Reasonable spin up time depend on the spatial scale of the model: For regional and global models, the spin-up time can be on the order of days. For street canyon modelling, on the other hand, 30 minutes have been considered conservative (Bright, 2012).

2.4. Target compound sets

Depending on the goal of a simulation, different compounds are of interest. In this study we perform mechanism reduction constrained to two target compound sets, to investigate the influence on the mechanism size and its composition of reactions. The two sets of target compounds are:

- *Emmerson*: Emmerson and Evans (2009) studied the concentrations of ozone, NO_x, nitrate, hydroxyl radical, and PAN for a number of mechanisms. In the present study, these compounds make up the *Emmerson* target compound set with the expansion of NO_x into nitric oxide and nitrogen dioxide. Nitric oxide and nitrogen dioxide are thus targeted individually in the reduction process, even though occasionally represented together as NO_x.

- *Basic*: Ozone, nitric oxide, and nitrogen dioxide are arguably the compounds of most interest in the air pollution community, partly due to their environmental and health impacts, partly to the extensive monitoring of these compounds in urban settings. These compounds constitute the *Basic* target compound set.

2.5. Reaction categories

In the analysis of the generated mechanisms seven mutually exclusive categories of reactions are used. There is a hierarchy of the categories, such that

12

those reactions that meet the criteria of several categories, fall in the first cate-
gory for which these criteria is met, as they are listed below:

1. *RO_2 + NO*: All the reactions in the form $RO_2 + NO \longrightarrow RO + NO_2$, where an organic peroxy radical reacts with a nitric oxide to produce a nitrogen dioxide.

2. *RH + OH*: All the reactions in the form $RH + OH \xrightarrow{O_2} RO_2 + H_2O$, where an organic compound reacts with a hydroxyl radical to eventually produce an organic peroxy radical.

3. *other NO_x*: Other reactions that have nitric oxide or nitrogen dioxide either as a reactant or a product.

4. *other NO_y*: Other reactions that have any nitrogen containing compound (predominantly oxidized nitrogen, commonly defined as $[NO_y] \equiv [NO_x]$ + $[HNO_3]$ + $[HONO]$ + $[N_2O_5]$ + $[ClONO_2]$ + $[NO_3]$ + $[HOONO_2]$ + $[BrONO_2]$), either as a reactant or a product. However, all reactions involving nitric oxide or nitrogen dioxide fall into the *other NO_x* category and are not included here. This reaction category is especially associated with night time chemistry.

5. *other HO_x*: Other reactions that have hydroxyl radical or hydroperoxyl radical either as a reactant or a product.

6. *other RO_2*: Other reactions that have an organic peroxy radical either as a reactant or a product (predominantly peroxy-peroxy reactions).

7. *other*: All other reaction (O_x reactions and unimolecular decomposition of hydrocarbons).

The reaction categories are designed to capture the characteristics of mechanisms beyond size.

3. Results and discussion

3.1. Different pollution scenarios

The size and the score of all simulations with the A0.90 (A0.70) mechanism of all the cases, as described in Sections 2.1 and 2.2, are tabulated in Table

13

2. The extent of reduction in number of reactions and species for the reduced mechanisms, including the *all-round* mechanism, are presented in Table 3. All reduced mechanisms are developed for five simulated days using the *Emmerson* target compound set except where otherwise noted. The threshold for the accuracy based mechanism in the *biogenic* case is lowered to 0.70 (A0.70), since the method does not return useful mechanisms with accuracy above 0.90 with the current settings. The smallest A0.90 mechanism for the *biogenic* case generated thus far includes 1734 reactions and 633 species. The partial scores of the A0.90 (A0.70) mechanisms are presented in see Table 4.

Since common approaches to chemistry simulations of urban street canyon air quality models are either to use a minimal O_3–NO_x-mechanism (Zhong et al., 2016a) or simply regard all compounds as unreactive (no chemistry) (Vardoulakis et al., 2003), the cases are tested with these approaches. Scores obtained by simulations with an O_3–NO_x mechanism, covering only three reactions, and scores calculated by keeping the concentrations constant (no chemistry) are tabulated in Table 2.

It can be deduced from Tables 2–4 that the method can successfully generate reduced mechanisms for simple non-isoprene or isoprene lean atmospheric chemistry cases, down to a third or even a tenth the size of a near-explicit chemistry subset without losing more than 10 % accuracy on average of predictions of a set of relevant compounds over at least as long as five days, even if the chemistry is in the NO_x-limited regime. Isoprene rich chemistry proved to require larger numbers of reactions to accurately predict the target compound concentrations, especially PAN and hydroxyl radicals (both with partial scores of 0.54 for the A0.70). The *all-round mechanisms* scored 0.98 or higher for all non-isoprene cases, 0.90 for the *industrial* case, and 0.56 for the *biogenic case*.

Generally, the score of the cases with $\mu(L_N/Q) < 0.5$ (*hot & wet*, *clean*, and *biogenic*) are mostly held back by the low accuracy of the PAN prediction, while this is not the case for the cases with higher $\mu(L_N/Q) > 0.5$, where the PAN score does not stand out from the other trace gas species prediction scores.

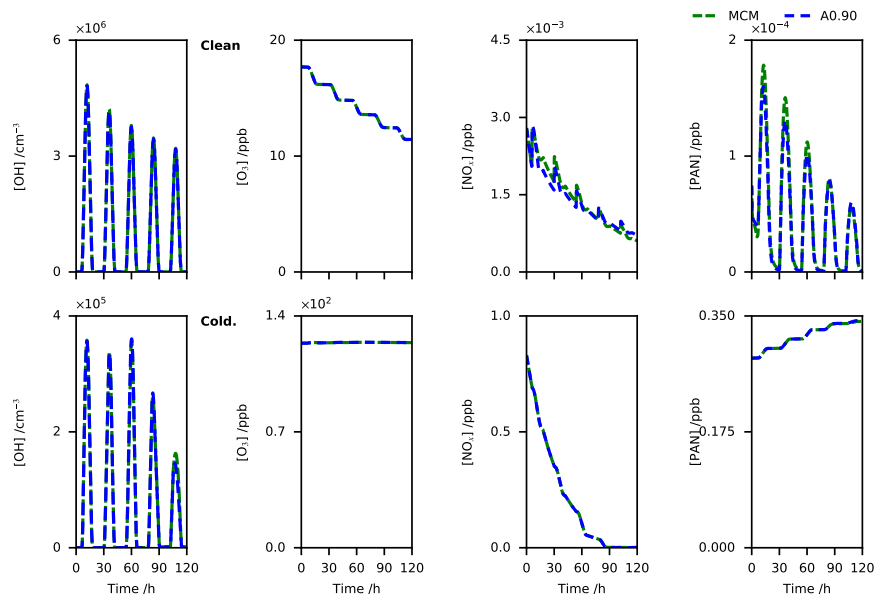### 3.2. Non-isoprene cases

3.2.1. Cases

Figure 2: Details of the simulation of the *clean* (upper panels) and *cold & dry* (lower panels) over five days: MCM (green color) and A0.90 mechanisms (blue) broken up compound by compound as (from left) OH, O_3, NO_x, and PAN. All mechanisms are optimized to simulate the *Emmerson* target compound set. The scoring is described in Eq. (1).

³³⁵ The result of all non-isoprene cases, five-day simulations with the A0.90 mechanism of all the cases are depicted along with the results of the simulation using the non-isoprene MCM subset in Figs. 2 and 3, all developed using the *Emmerson* target compound set. The result of the high NO_x alteration of the *hot & wet* case five-day simulation is depicted in Fig. 4. Additionally, the scores of the prediction of peroxy radical concentrations ($[HO_2]$ and $[RO_2]$) of the five-day *Emmerson* non-isoprene mechanism simulations are added to Table 4. The time resolved concentration predictions are plotted in Figs. S.14–S.18 in the Supplementary Material.

Figs. 2 and 3 show very small deviations between the reduced mechanisms ³⁴⁵ and the full MCM predictions. The reactions included in the A0.90-mechanisms,
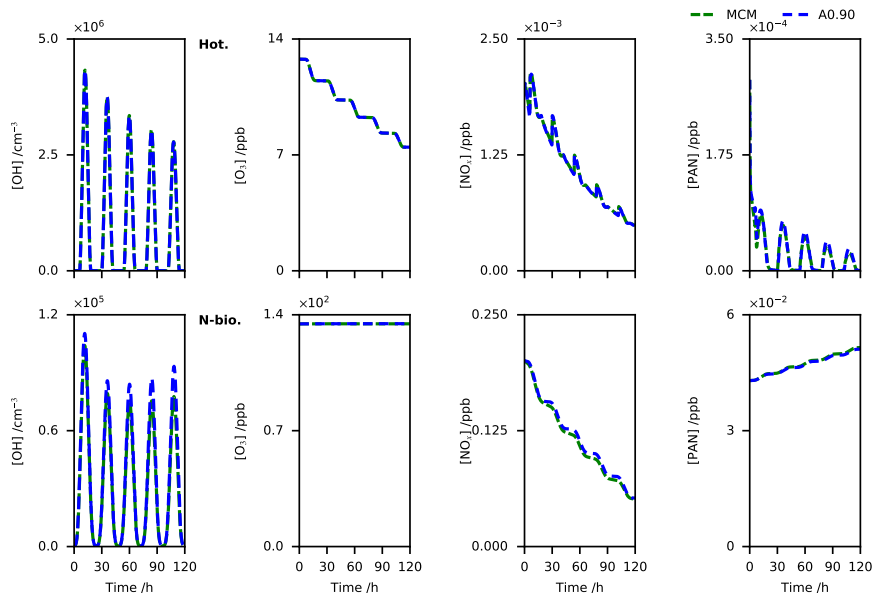
15

Figure 3: Details of the simulation of the *hot & wet* (upper panels) and *non-biogenic* (lower panels) over five days: MCM (green color) and A0.90 mechanisms (blue) broken up compound by compound as (from left) OH, O_3, NO_x, and PAN. All mechanisms are optimized to simulate the *Emmerson* target compound set. The scoring is described in Eq. (1).

divided into the reaction categories as defined in Section 2.5 are depicted as bars in Fig. 5, the number of reactions of each category in the MCM subset are depicted as envelope bars. For all the cases the largest absolute reduction is in the *other HO_x* category (where 73–94 reactions are removed from the MCM sub-

350 set corresponding to 36 %–39 % of the total reduction), followed by the *other NO_x* (53–61 reactions corresponding to 23 %–28 %), *other RO_2* (31–40 reactions, corresponding to 15 %–18 %), *RH + OH* (19–30 reactions corresponding to 11 %–12 %), *RO_2 + NO* (10–13 reactions, corresponding to 4 %–5 %), *other NO_y* (8–10 reactions, corresponding to about 4 %), and *other* (3 reactions, cor-

355 responding to 1 %–2 %) categories. About a third of the reduction in any of the cases investigated are thus made in the categories concerning hydrocarbons (*RO_2 + NO*, *RH + OH*, and *other RO_2*), about a third in the category concerning HO_x reactions without hydrocarbons (*other HO_x*), and about a third
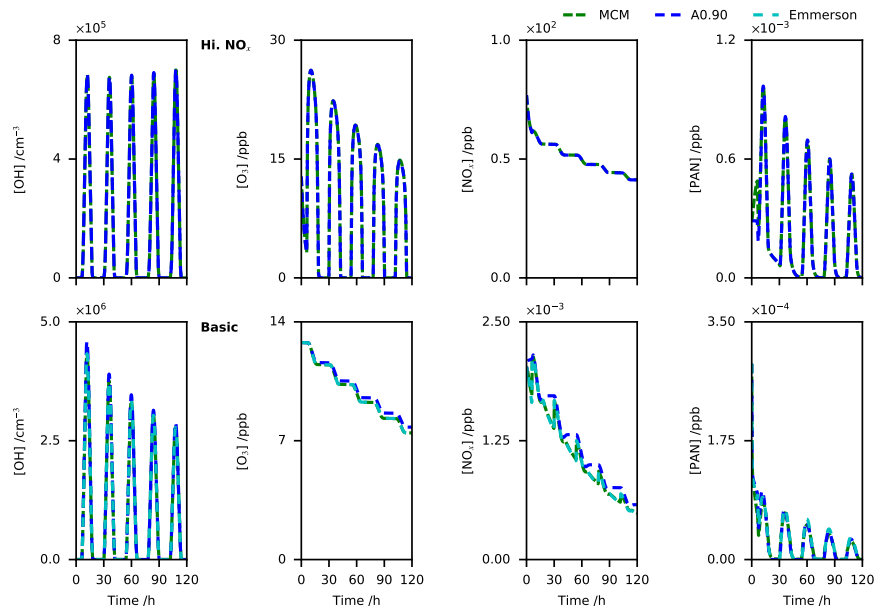
16

Figure 4: Details of the simulation of the *hot & wet, high NO_x* (upper panels) and *hot & wet, Basic target set* (lower panels) over five days: MCM (green color) and A0.90 mechanisms (blue) broken up compound by compound as (from left) OH, O_3, NO_x, and PAN. In the lower panel the *Emmerson* target set A0.90 is included for comparison (cyan). The scoring is described in Eq. (1).

in the categories concerning reactions including reactive nitrogen without hy-

360 drocarbons (*other NO_x* and *other NO_y*). Only a small reduction is made in the *other* category. The absolute reduction scales quite well with the size of the category in the MCM subset: The more reactions that are included in the category, the more reactions are removed by the reduction process. It can be noted, however, that the *other NO_y* (9 %–27 % of the reactions are left), *other HO_x*

365 (11 %–31 %), and *other RO_2* (2 %–24 %) categories are generally reduced to a higher degree than the *RO_2 + NO* (18 %–37 %), *RH + OH* (14 %–45 %), and *other NO_x* (22 %–32 %) categories for the selected mechanisms. All the A0.90 mechanism have the same set of *other* reactions, which are the oxygen/ozone regeneration reactions and the decomposition of formaldehyde. The oxygen/ozone

370 regeneration reactions have in the current reduction processes been included in

17

the mechanisms automatically and were therefore not explicitly selected by the reduction process. The relatively small size of the *non-biogenic* mechanism implies that the general level of initial concentrations of the reactants, not only their relative abundance, influence the extent of reduction. This could be the result of smaller variation in reaction channels.

Indication on how the NO_x regime affects the reduction process can be easiest found by comparing the *hot & wet* and the *hot & wet, high NO_x* cases since only the NO_x content differs between the two. The reduction process did render a smaller A0.90 mechanism for the *hot & wet, high NO_x* than the default *hot & wet* case (57 reactions, 38 species versus 96 reactions, 57 species). The partial scores (Table 4) give relatively better PAN scores (0.92 for the high NO_x versus 0.80 for the default *hot & wet* case). Regarding the composition of reaction categories, Fig. 5 shows that the largest relative difference between *hot & wet* and *hot & wet, high NO_x* are in the *other RO_2* (24 % versus 4 %), *RH + OH* (45 % versus 20 %), and *other HO_x* (31 % versus 11 %) categories, where the high NO_x case is more reduced. The reduction rate is identical for the *RO_2 + NO* (37 %), *other NO_x* (29 %), and *other* (62 %) categories. The default *hot & wet* case is slightly less reduced for the *other NO_y* category (27 % versus 18 %) than the high NO_x case. HO_x and hydrocarbon chemistry is thus less influential on the chemistry controlling the concentration of the target compounds in the high NO_x regime than in the low NO_x regime, in agreement with established literature (Jacob, 1999).

3.2.2. Time scales

To investigate the influence of time scale on the reduction process, two additional reduction processes are run for the *Emmerson* target compound set, *hot & wet* case with reduced times scales of one simulated day and one simulated hour, as described in Section 2.3, and the resulting predictions are depicted in Fig. 6. Additionally, the scores of the prediction of peroxy radical concentrations of the one-day and one-hour *Emmerson hot & wet* simulations are added to Table 4. The time resolved concentration predictions are plotted in Figs. S.19
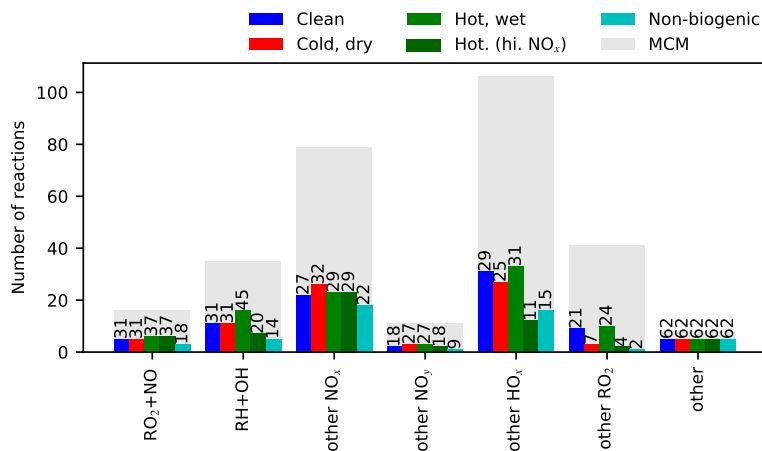
18

Figure 5: Number of reactions of the A0.90 mechanisms of the non-isoprene cases: *Clean* (blue color), *cold & dry* (red), *hot & wet* (light green), and *non-biogenic* (cyan) including the high NO_x alteration of the *hot & wet* case (dark green) five-day simulations generated by ACR for each reactions category with the *Emmerson* target compound set, the numbers above the bars represent the fraction of the numbers of reactions in the reduced mechanisms to the numbers of reactions in the MCM subset of each category, expressed in percent

and S.20 in the Supplementary Material.

The one-hour A0.90 mechanism is smaller (61 reactions, 36 species) than both the one-day mechanism (82 reactions, 49 species) and the five-day mechanism (96 reactions, 57 species). Averaged over all the four non-isoprene cases, generated one-day A0.90 mechanisms are reduced 11 % (three percentage points) more than corresponding generated five-day mechanisms (*Emmerson* target compound set). Generated one-hour A0.90 mechanisms are reduced 27 % (seven percentage points) more than the corresponding five-day mechanisms.

The largest difference in partial scores between the one-hour and one-day mechanisms of the target compounds are PAN where the one-day mechanism scores are better than the one-hour (0.79 versus 0.64), and the nitric oxide where
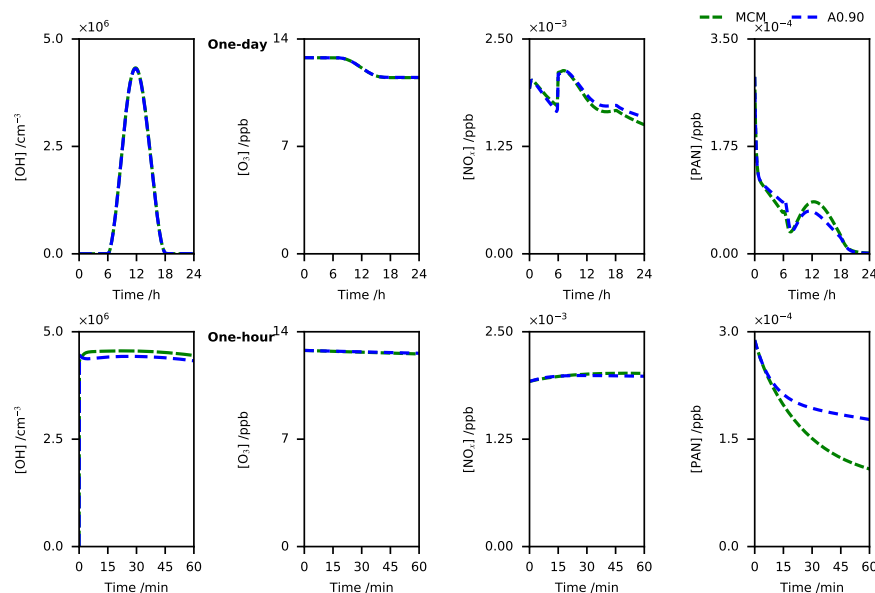
19

Figure 6: Details of simulations of the *hot & wet* case over three different time scales, the lines correspond to the full MCM simulations (green color), the A0.90 mechanisms with the *Emmerson* target compound set (blue), broken up compound by compound as (from left) OH, O_3, NO_x, and PAN. The scoring is described in Eq. (1).

the one-hour mechanism scores higher than the one-day mechanism (0.96 versus 0.88). Both mechanisms score worse than the five-day mechanism for nitrate (0.85 versus 0.93). It should be noted, however, that nitrate is associated with

⁴¹⁵ night time chemistry and is therefore not particularly relevant for the one-hour case. The mechanisms, split up according to the reaction categories as defined in Section 2.5, are depicted as bars in Fig. 7. The one-day mechanism include a larger fraction of *other NO_x* and *other NO_y* reactions than the one-hour mechanism (26 % versus 21 % and 27 % versus 9 % respectively), reflecting the need

⁴²⁰ for a working night time chemistry in the one-day mechanism. Between the five-day mechanisms and the one-day mechanisms, the largest relative difference is in the $RO_2 + NO$ reactions (37 % versus 18 %). This is presumably due to the twelwe percentage points larger contribution of organic peroxy radicals from the oxidation of the more long lived organic carbons especially with life-
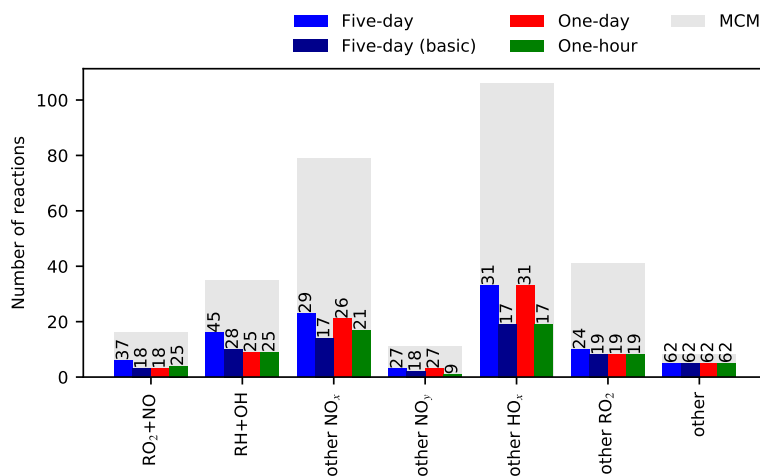
20

Figure 7: Number of reactions of the A0.90 mechanisms of the *hot & wet* case over three different time scales: Five-day (light blue color), one-day (red), one-hour (green) for each reactions category with the *Emmerson* target compound set along with the five-day *Basic* target compound set mechanism (dark blue), the numbers above the bars represent the fraction of the numbers of reactions in the reduced mechanisms to the numbers of reactions in the MCM subset of each category, expressed in percent

425 times on the order of days (mainly methylperoxy radical CH_3O_2 reformed from methylhydroperoxid CH_3OOH), in the five-day simulations, see Fig. 8.

3.2.3. Target compounds

To test the influence of the choice of target compounds on the reduction process, a reduction was made for the five-day *hot & wet* case with the *Ba-* 430 *sic* target compound set in addition to the *Emmerson* target compound set, as described in Section 2.4, and the resulting predictions depicted in Fig. 4. Additionally, the scores of the prediction of peroxy radical concentrations of the five-day *Basic hot & wet* mechanism simulations are added to Table 4. The time resolved concentration predictions are plotted in Fig. S.21 in the Supplementary 435 Material.
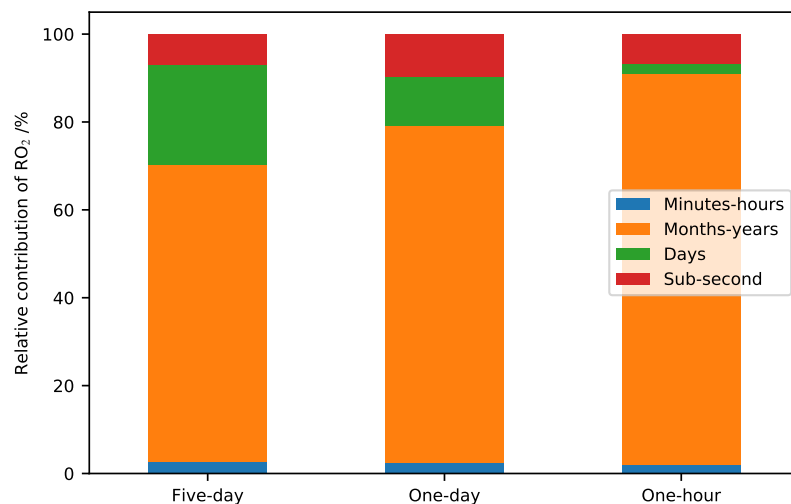
21

Figure 8: The relative contribution of organic peroxy radical production from reactions with RO_2 precursors with lifetimes on the time scale of month to years (orange), days (green), minutes to hours (blue), and under a second (red) for the five-day, one-day, and one-hour base simulations respectively

The *Basic* A0.90 mechanism is substantially smaller (61 reactions, 36 species) than the corresponding *Emmerson* mechanism (96 reactions, 57 species). Averaged over all the four non-isoprene cases, generated *Basic* A0.90 mechanisms are reduced 18 % (five percentage points) more than the corresponding *Emmerson* mechanisms (five-day).

The largest difference between the two mechanisms of the *Emmerson* target compounds are nitrate (0.93 verus 0), for which the concentrations collapses in the *Basic* mechanisms. The hydroxyl radical concentrations are quite well represented in the *Basic* mechanism (0.89) even if it is not included in the target compound sets. The most visually obvious deviation between the curves in Fig. 4 is arguably the night time behavior of NO_x, which is probably connected to the missing nitrate chemistry. It can be noted that the method seems guided by the inclusion of nitrate in the target compound set towards better NO_x

22

concentration predictions. The number of reactions in each of the reaction categories as defined in Section 2.5 included in the five-day *hot & wet Basic* mechanism are plotted as a barplot in Fig. 7. The use of the *Basic* target compound set result in mechanisms most reduced in the *other NO_x* and the *other HO_x* (both 17 % of the MCM subset) and the *$RO_2 + NO$* and *other NO_y* categories (both 18 %). It is less reduced for the *RH + OH* categories (28 %). The mechanism is not further reduced in the *other* category (predominantly O_x chemistry) than any other mechanism (62 %). Relative to the corresponding *Emmerson* target set mechanism the *Basic* mechanism is most reduced in the *$RO_2 + NO$* (19 percentage points lower than the *Emmerson* mechanism) and *RH + OH* (17 percentage points lower). The *Basic* mechanism is relative to the corresponding *Emmerson* mechanism less reduced in the *other RO_2* (five percentage points) and *other NO_y* (nine percentage points) categories.

The results from the reductions of the two different target set mechanisms imply that the size of a reduced mechanism can depend on the compounds of interest; if only ozone and NO_x concentrations are of interest, parts of the chemistry can be left out without substantially compromising the accuracy of the predictions of these compounds' concentrations.

3.3. Isoprene cases

The result of the isoprene case simulations (five-day, *Emmerson* target compound set) along with the results of the corresponding simulations using the MCM subset including isoprene are plotted in Fig. 9. Additionally, the scores of the prediction of peroxy radical concentrations of the five-day *Emmerson industrial* and *biogenic* mechanism simulations are added to Table 4. The time resolved concentration predictions are plotted in Figs. S.22 and S.23 in the Supplementary Material.

The A0.90 (*industrial*) and the A0.70 (*biogenic*) mechanisms are split up according to the reaction categories as defined in Section 2.5 and are depicted as bars in Fig. 10 along with the *all-round* mechanism and the *hot & wet* mechanism, which represents a non-isoprene mechanism. The largest relative differ-
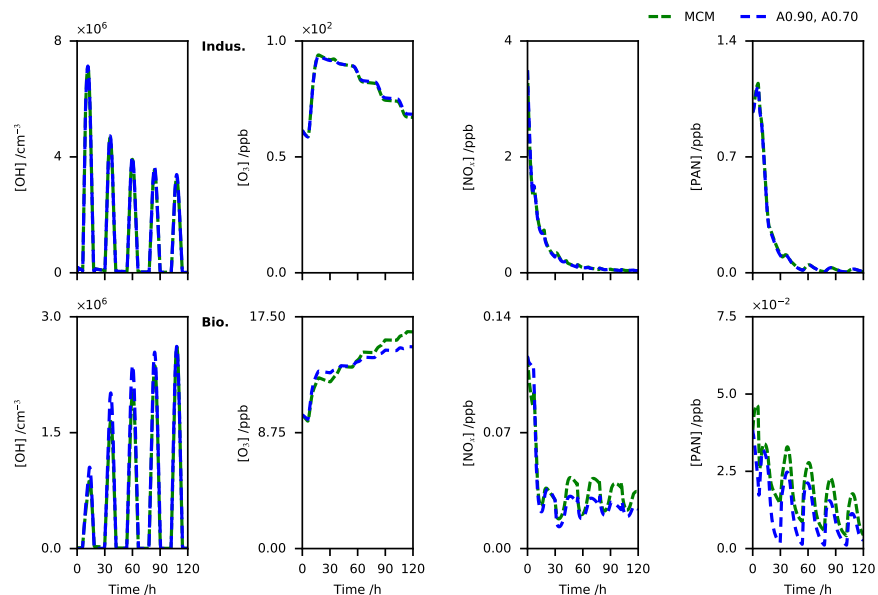
23

Figure 9: Details of the simulation of the isoprene cases over five days, the full MCM and A0.90 mechanisms (A0.70 for *biogenic* case) of the case category generated by ACR (blue) broken up compound by compound as (from left) OH, O_3, NO_x, and PAN. All mechanisms are optimized to simulate the *Emmerson* target compound set. The scoring is described in Eq. (1).

ence between the *biogenic* case (isoprene rich) and *industrial* (isoprene lean) is in
480   the $RO_2 + NO$ category where the *biogenic* case mechanism include 45 % of the
$RO_2 + NO$ type reactions, while the *industrial* case mechanism includes 10 %.
Even the large *all-round* mechanism does not include more than 27 %. The
reason for this is probably the elevated levels of isoprene yielding more organic
peroxy radicals. The difference in composition of reaction categories between
485   the *industrial* case and the *hot & wet* case are small (0–10 percentage points).
Not only the compositions of reactants, but also their initial concentration will
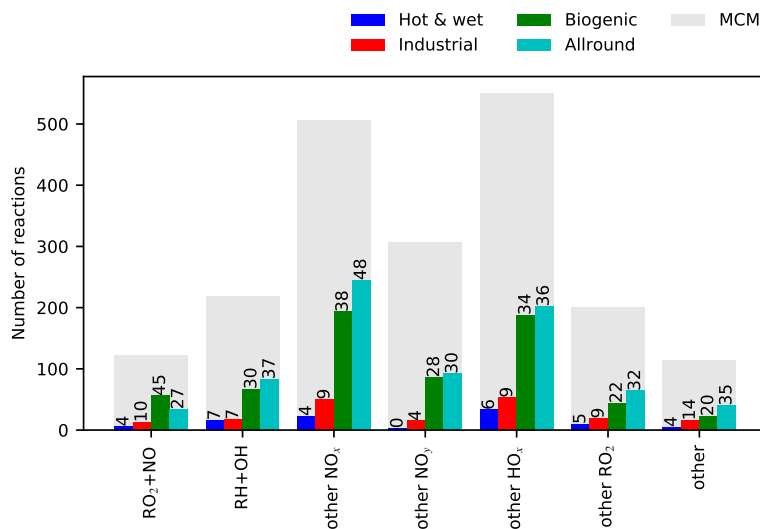thus influence the reduction.

24

Figure 10: Number of reactions of the A0.90 mechanisms of the five-day simulations of the *hot & wet* case (blue color) compared to the two isoprene cases: *Industrial* (red), *biogenic* (green), and *all-round* (cyan) generated by ACR for each reactions category with the *Emmerson* target compound set, the numbers above the bars represent the fraction of the numbers of reactions in the reduced mechanisms to the numbers of reactions in the MCM subset of each category, expressed in percent. Note that the *hot & wet* case here is compared to the MCM subset including isoprene, hence the deviation from the numbers presented in Figs. 5 and 7.

4. Conclusions and Outlook

Reduced mechanisms generated by the Ant Colony Reduction (ACR) method
490 are here proven able to successfully predict ozone, nitrogen oxides, and other important compounds' concentrations in simulations of several cases up to five simulated days. The mechanisms typically include 10 %–30 % of all reactions in the relevant subset of the detailed chemical kinetic mechanism (MCM v3.3.1).

The extent of the reduction depends on the time scale, the composition and
495 initial concentration of reactants, NO_x regime, and the compounds of interest. Smallest mechanisms are obtained for cases on shorter time scales with fewer compounds (especially reactive hydrocarbons such as isoprene), lower initial

concentrations, and fewer compounds of interest. High NO_x cases result in smaller mechanisms compared to low NO_x cases. It is also shown here that these different conditions require different parts of the chemistry; e.g. daytime simulations deselects NO_y reactions to a larger degree than simulations with time scales on the order of days, longer time scales require more $RO_2 + NO \longrightarrow RO + NO_2$ type reactions, and higher NO_x cases require less hydrocarbon and HO_x chemistry.

Future developments include optimization of reaction rates and emission-, intermediate species-, and reaction lumping. Optimization of reaction rates will compensate loss of reactivity in deselected reactions by turning up the rate of other reactions which have a similar role in the chemistry. Emission lumping will enable reduced mechanisms for large number of hydrocarbons by joining groups of hydrocarbon into surrogate species. Intermediate species lumping will decrease the size of the mechanisms by joining intermediate species into surrogate species and reaction lumping by bypassing fast reaction steps.

The reduction method is very useful for time consuming simulations, e.g. street canyon CFD, where only a limited set of chemical reactions can be included. These environments have a limited complexity and therefore small mechanisms can be tailored without significant loss of accuracy. For climate modeling, where a wide range of species and conditions need to be included, the method extracts larger mechanisms. The use of the method for creating mechanisms for a wide range of conditions will significantly benefit from implementation of further reduction strategies like reaction lumping.

Acknowledgements

Bey, I., Jacob, D. J., Yantosca, R. M., Logan, J. A., Field, B. D., Fiore, A. M., Li, Q., Liu, H. Y., Mickley, L. J., Schultz, M. G., 2001. Global modeling of tropospheric chemistry with assimilated meteorology: Model description and evaluation. Journal of Geophysical Research: Atmospheres 106 (D19), 23073–23095.

Bright, V. B., 2012. Street canyon atmospheric composition: Coupling dynamics and chemistry. Ph.D. thesis, University of Birmingham.

Bright, V. B., Bloss, W. J., Cai, X., 2013. Urban street canyons: Coupling dynamics, chemistry and within-canyon chemical processing of emissions. Atmospheric Environment 68, 127–142.

Carter, W. P., 2010. Development of the saprc-07 chemical mechanism. Atmospheric Environment 44 (40), 5324–5335.

Carter, W. P., Heo, G., 2013. Development of revised saprc aromatics mechanisms. Atmospheric environment 77, 404–414.

Chen, S., Ren, X., Mao, J., Chen, Z., Brune, W. H., Lefer, B., Rappenglück, B., Flynn, J., Olson, J., Crawford, J. H., 2010. A comparison of chemical mechanisms based on tramp-2006 field data. Atmospheric Environment 44 (33), 4116–4125.

Damian, V., Sandu, A., Damian, M., Potra, F., Carmichael, G. R., 2002. The kinetic preprocessor KPP-a software environment for solving chemical kinetics. Computers & Chemical Engineering 26 (11), 1567–1579.

Dorigo, M., Birattari, M., 2011. Ant colony optimization. In: Encyclopedia of machine learning. Springer, pp. 36–39.

Dorigo, M., Maniezzo, V., Colorni, A., 1996. Ant system: optimization by a colony of cooperating agents. IEEE Transactions on Systems, Man, and Cybernetics, Part B (Cybernetics) 26 (1), 29–41.

Emmerson, K., Carslaw, N., 2009. Night-time radical chemistry during the torch campaign. Atmospheric Environment 43 (20), 3220–3226.

Emmerson, K., Evans, M., 2009. Comparison of tropospheric gas-phase chemistry schemes for use within global models. Atmospheric Chemistry and Physics 9 (5), 1831–1845.

Emmons, L. K., Walters, S., Hess, P. G., Lamarque, J.-F., Pfister, G. G., Fillmore, D., Granier, C., Guenther, A., Kinnison, D., Laepple, T., et al., 2010. Description and evaluation of the model for ozone and related chemical tracers, version 4 (mozart-4).

EPA, 2011. Air quality index for nitrogen dioxide. [ONLINE].
URL https://www3.epa.gov/airnow/no2.pdf

Gery, M. W., Whitten, G. Z., Killus, J. P., Dodge, M. C., 1989. A photochemical kinetics mechanism for urban and regional scale computer modeling. Journal of Geophysical Research: Atmospheres 94 (D10), 12925–12956.

Ginnebaugh, D. L., Liang, J., Jacobson, M. Z., 2010. Examining the temperature dependence of ethanol (E85) versus gasoline emissions on air pollution with a largely-explicit chemical mechanism. Atmospheric Environment 44 (9), 1192–1199.

IPCC, 2013. Summary for Policymakers. Cambridge University Press, Cambridge, United Kingdom and New York, NY, USA, book section SPM, p. 130.
URL www.climatechange2013.org

Jacob, D., 1999. Introduction to atmospheric chemistry. Princeton University Press.

Jenkin, M., Saunders, S., Wagner, V., Pilling, M., 2003. Protocol for the development of the master chemical mechanism, mcm v3 (part b): tropospheric degradation of aromatic volatile organic compounds. Atmospheric Chemistry and Physics 3 (1), 181–193.

Jenkin, M., Watson, L., Utembe, S., Shallcross, D., 2008. A Common Representative Intermediates (CRI) mechanism for VOC degradation. Part 1: Gas phase mechanism development. Atmospheric Environment 42 (31), 7185–7195.

Jenkin, M., Young, J., Rickard, A., 2015. The MCM v3.3.1 degradation scheme for isoprene. Atmospheric Chemistry & Physics 15 (20).

Junier, M., Kirchner, F., Clappier, A., van den Bergh, H., 2005. The chemical mechanism generation programme CHEMATA–Part 2: Comparison of four chemical mechanisms for mesoscale calculation of atmospheric pollution. Atmospheric Environment 39 (6), 1161–1171.

Kim, M. J., Park, R. J., Kim, J.-J., 2012. Urban air quality modeling with full O_3–NO_x–VOC chemistry: Implications for o 3 and pm air quality in a street canyon. Atmospheric Environment 47, 330–340.

Kirchner, F., 2005. The chemical mechanism generation programme CHEMATA–Part 1: The programme and first applications. Atmospheric Environment 39 (6), 1143–1159.

Kleinman, L. I., Daum, P. H., Lee, J. H., Lee, Y.-N., Nunnermacker, L. J., Springston, S. R., Newman, L., Weinstein-Lloyd, J., Sillman, S., 1997. Dependence of ozone production on no and hydrocarbons in the troposphere. Geophysical Research Letters 24 (18), 2299–2302.

Madronich, S., Calvert, G., 1989. The NCAR Master Mechanism of the gas phase chemistry-version 2.0.

MCM, 2018. The Master Chemical Mechanism. [ONLINE].
URL http://mcm.leeds.ac.uk/MCMv3.3.1/home.htt

Monks, P., Granier, C., Fuzzi, S., Stohl, A., Williams, M., Akimoto, H., Amann, M., Baklanov, A., Baltensperger, U., Bey, I., et al., 2009. Atmospheric composition change–global and regional air quality. Atmospheric Environment 43 (33), 5268–5350.

Naik, V., Voulgarakis, A., Fiore, A. M., Horowitz, L. W., Lamarque, J.-F., Lin, M., Prather, M. J., Young, P., Bergmann, D., Cameron-Smith, P., et al., 2013. Preindustrial to present-day changes in tropospheric hydroxyl radical and methane lifetime from the atmospheric chemistry and climate model inter-comparison project (ACCMIP). Atmospheric Chemistry and Physics 13 (10), 5277–5298.

NCAR, 2018. Atmospheric chemistry observation and modelling. [ONLINE].
URL https://www2.acom.ucar.edu/modeling/ncar-master-mechanism

Pichler, C. S., Nilsson, E. J. K., 2018. Reduced kinetic mechanism for methanol combustion in spark-ignition engines. Energy & Fuels.

Roldin, P., Eriksson, A., Nordin, E., Hermansson, E., Mogensen, D., Rusanen, A., Boy, M., Swietlicki, E., Svenningsson, B., Zelenyuk, A., et al., 2014. Modelling non-equilibrium secondary organic aerosol formation and evaporation with the aerosol dynamics, gas-and particle-phase chemistry kinetic multilayer model ADCHAM. Atmospheric Chemistry and Physics 14 (15), 7953–7993.

Sanchez, B., Santiago, J.-L., Martilli, A., Palacios, M., Kirchner, F., 2016. CFD modeling of reactive pollutant dispersion in simplified urban config-urations with different chemical mechanisms. Atmospheric Chemistry and Physics 16 (18), 12143–12157.

SAPRC, 2013. Atmospheric chemical mechanisms and voc reactivity scales. [ONLINE].
URL https://www.cert.ucr.edu/~carter/SAPRC/

Saunders, S. M., Jenkin, M. E., Derwent, R., Pilling, M., 2003. Protocol for the development of the Master Chemical Mechanism, MCM v3 (Part A): tropo-spheric degradation of non-aromatic volatile organic compounds. Atmospheric Chemistry and Physics 3 (1), 161–180.

Stockwell, W. R., Kirchner, F., Kuhn, M., Seefeld, S., 1997. A new mecha-

30

nism for regional atmospheric chemistry modeling. Journal of Geophysical Research: Atmospheres 102 (D22), 25847–25879.

Vardoulakis, S., Fisher, B. E., Pericleous, K., Gonzalez-Flesca, N., 2003. Modelling air quality in street canyons: a review. Atmospheric Environment 37 (2), 155–182.

Watson, L., Shallcross, D., Utembe, S., Jenkin, M., 2008. A Common Representative Intermediates (CRI) mechanism for VOC degradation. Part 2: Gas phase mechanism reduction. Atmospheric Environment 42 (31), 7196–7204.

Wennberg, P. O., Bates, K. H., Crounse, J. D., Dodson, L. G., McVay, R. C., Mertens, L. A., Nguyen, T. B., Praske, E., Schwantes, R. H., Smarte, M. D., et al., 2018. Gas-phase reactions of isoprene and its major oxidation products. Chemical reviews 118 (7), 3337–3390.

Whalley, L., Edwards, P., Furneaux, K., Goddard, A., Ingham, T., Evans, M., Stone, D., Hopkins, J., Jones, C. E., Karunaharan, A., et al., 2011. Quantifying the magnitude of a missing hydroxyl radical source in a tropical rainforest. Atmospheric Chemistry and Physics 11 (14), 7223–7233.

WHO, 2006. Air quality guidelines for particulate matter, ozone, nitrogen dioxide and sulfur dioxide-global update 2005-summary of risk assessment, 2006. Geneva: WHO.

Yarwood, G., Jung, J., Whitten, G. Z., Heo, G., Mellberg, J., Estes, M., 2010. Updates to the carbon bond mechanism for version 6 (cb6). In: 2010 CMAS Conference, Chapel Hill, NC. October.(http://www. cmascenter. org/conference/2010/abstracts/emery_updates_carbon_2010. pdf).

Zhong, J., Cai, X.-M., Bloss, W. J., 2016a. Coupling dynamics and chemistry in the air pollution modelling of street canyons: a review. Environmental Pollution 214, 690–704.

Zhong, J., Cai, X.-M., Bloss, W. J., 2016b. Modelling photochemical pollu-
tants in a deep urban street canyon: Application of a coupled two-box model
approximation. Atmospheric Environment 143, 86–107.

665

Table 1: Initial values of the test cases as described previously (Emmerson and Evans, 2009), initial concentrations are given in ppb

Init. val.	Indus.	Clean	Cold.	Hot.	Bio.	Non-bio.
Lon. /°E	100	-120	-5	-140	-145	-160
Lat. /°N	18	-30	-6	-10	26	-75
Date (mm-dd)	4-14	2-14	10-11	12-10	7-13	12-31
Press. /hPa	982.6	941.6	1036.6*	982.6	982.6	1036.6*
Temp. /K	299.7	299.4	214.4	302.7	302.5	214.3
Rel. hum. /%	46	71	152	71	57	154
CH_4	1700.0	1700.0	1700.0	1700.0	1700.0	1700.0
CO	956.5	58.4	87.6	56.9	217.7	56.1
NO_2	3.6	0.003	0.58	0.002	0.12	0.14
(high NO_x)				80.0		
O_3	63.3	19.0	86.3	13.3	10.5	93.9
H_2O_2	11.0	1.7	0.05	1.5	8.5	0.02
HNO_3	2.8	0.003	0.58	0.002	0.12	0.14
C_2H_6	5.6	0.2	0.9	0.2	0.6	0.3
C_3H_8	1.4	0.003	0.2	0.002	0.09	0.02
C_5H_8	0.3	–	–	–	6.7	–
HCHO	6.0	0.4	0.06	0.4	4.8	0.02
CH_3CHO	3.0	0.004	0.007	0.004	3.8	0.0006
CH_3COCH_3	17.9	1.5	2.0	1.5	15.4	0.36
PAN	1.0	0.00008	0.2	0.0003	0.04	0.03
$\mu(L_N/Q)$	0.52	0.34	0.66	0.34	0.40	0.55
(high NO_x)				0.98		

*The original pressure values are treated as misprint

Table 2: Size (number of reactions) and score of the A0.90 mechanisms, the O_3–NO_x column reflect the corresponding score obtained with a minimal photostationary state scheme, the *No chem.* column reflect the corresponding score obtained with constant concentrations. The scoring is described in Eq. (1).

Case	A0.90		O_3–NO_x	No chem.
	Size	Score		
Non-isoprene				
Clean	85	0.91	-0.14	-0.22
Non-biogenic	49	0.93	0.06	0.15
Cold & dry	80	0.91	-0.17	0.15
Hot & wet	96	0.94	-0.07	-0.2
high NO_x	57	0.97	-0.11	-0.41
basic	61	0.90	-0.15	-0.13
one-day	82	0.91	0.37	0.08
one-hour	63	0.90	0.37	0.23
Isoprene				
Industrial	183	0.95	-0.21	-0.21
Biogenic	657*	0.74*	-0.19	-0.21
All-round	760	0.90	-0.12	-0.09

*A0.70

Table 3: Number of reactions (*Reac.*) and species (*Spec.*) of the A0.90 mechanisms and of their corresponding base mechanism (*Base mech.*), and the fraction $n_{\mathrm{A0.90}}/n_{\mathrm{base}}$ in % (*Rel. size*), where n either is the number of reactions (*Reac.*) or the number of species (*Spec.*) for the A0.90 and the base mechanism respectively.

Case	A0.90		Base mech.		Rel. size /%	
	Reac.	Spec.	Reac.	Spec.	Reac.	Spec.
Non-isoprene						
Clean	85	46	296	99	28.7	46.5
Non-biogenic	49	33	296	99	16.6	33.3
Cold & dry	80	49	296	99	27.0	49.5
Hot & wet	96	57	296	99	32.4	57.6
high NO_x	57	38	296	99	19.3	38.4
basic	61	36	296	99	20.6	36.4
one-day	82	49	296	99	27.7	49.5
one-hour	63	38	296	99	21.2	38.4
Isoprene						
Industrial	183	111	2016	638	9.1	17.4
Biogenic	657*	398*	2016	638	32.5	62.4
All-round	760	380	2016	638	37.7	59.6

*A0.70

Table 4: Partial and total score of the A0.90 (A0.70) mechanisms for the different cases. The scoring is described in Eq. (1).

Case	O_3	NO	NO_2	NO_3	OH	PAN	Tot.	HO_2	RO_2
Non-isoprene									
Clean	1.00	0.91	0.91	0.90	0.98	0.78	0.91	0.75	0.64
Non-biogenic	1.00	0.96	0.96	0.80	0.89	0.99	0.93	0.94	-1.0
Cold & dry	1.00	0.87	0.88	0.89	0.84	1.00	0.91	0.84	-1.0
Hot & wet	1.00	0.99	0.99	0.93	0.99	0.80	0.95	0.99	0.99
high NO_x	0.99	0.99	1.00	0.97	0.95	0.92	0.97	0.70	-1.0
basic	0.97	0.87	0.86	0.00	0.89	0.40	0.67†	0.32	-0.42
one-day	1.00	0.88	0.96	0.85	0.97	0.79	0.91	0.63	0.69
one-hour	1.00	0.96	0.99	0.85	0.97	0.64	0.90	0.99	0.89
Isoprene									
Industrial	0.99	0.97	0.97	0.94	0.91	0.96	0.96	0.85	0.67
Biological*	0.96	0.83	0.79	0.79	0.54	0.54	0.74	0.65	0.35
All-round	0.97	0.92	0.92	0.79	0.88	0.93	0.90	0.90	0.46

†The score is the average of all the partial scores, except HO_2 and RO_2

*A0.70